Published by Avanti Publishers

International Journal of Petroleum Technology

ISSN (online): 2409-787X

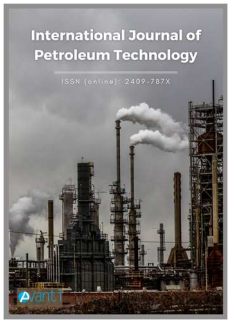

Permeability Prediction and Validation Using Static and Dynamic Data of Sandstone Reservoir in Weizhou Oilfield, Beibuwan Basin, China

Jian Wang[1], Hui Zhang[1], Huashan Jiang[2] and Lin Pan[3,*]

[1]*Sinopec Jianghan Oilfield Company, Wuhan, 430000, China*

[2]*Sinopec Northwest Oilfield Company, Urumqi, 830011, China*

[3]*China University of Geosciences, Wuhan, 430074, China*

ARTICLE INFO

Article Type: Research Article

Keywords:
Dynamic Data
Weizhou Oilfield
Geological Parameters
Well Log Interpretation
Permeability Prediction

Timeline:
Received: May 31, 2021
Accepted: June 21, 2021
Published: July 03, 2021

Citation: Wang J, Zhang H, Jiang H and Pan L. Permeability prediction and validation using static and dynamic data of sandstone reservoir in Weizhou Oilfield, Beibuwan Basin, China. Int J Petrol Technol. 2021; 8: 1-14.

DOI: https://doi.org/10.15377/2409-787X.2021.08.1

ABSTRACT

Permeability is one of the key parameters in reservoir property studies. The existing well log interpretation models could not predict the permeability accurately due to the complexity and ambiguity of well logging curves, and the prediction results may demonstrate significant contradictions with the production data. Based on the comprehensive analysis of cores, well logs, laboratory tests, and thin section observations, we take the first member of Liushagang Formation (L1) in Weizhou 11-1N Oil Field as the target, and select median grain size, porosity, and resistivity to establish a multiple nonlinear regression interpretation model of permeability. The accuracy and applicability of this model is validated by the laboratory test data and oil production performance. This permeability interpretation model is easy and practical to operate. Furthermore, it bridges the geological characteristics and the production performance.

*Corresponding Author
Email: panlin@cug.edu.cn
Tel: +8613807153269

1. Introduction

Permeability is one of the key parameters in reservoir physical property studies. Permeability could be obtained from laboratory tests, but the samples are too limited to give a whole image of the reservoir. Geophysical characteristics from well logs are employed to interpret the permeability. Resistivity has been a basic source of permeability interpretation since 1930s [1-3]. Porosity and water saturation are important properties which directly link to permeability. Brace tested a relation of permeability and formation factors, and the prediction result agreed to within about a factor of 2 over the 9 orders of magnitude range of permeability[4]; Jackson et al. investigated the relationship of formation factor and porosity[5]; Katz and Thompson presented an equation to calculate permeability from characteristic length (directly measured from mercury injection experiments) and brine conductivity[6, 7]; de Lima adopted an analytical approach to model the electrical properties of shaly sands and obtained water saturation and permeability from resistivity and porosity logs[8]. Along with the progress in computer science, new technical means, such as NMR, neural network, and fuzzy logic, have been explored to estimate permeability [9-22]. More advanced algorithms have been adopted and/or developed along with the fast development of data science and computer technics in recent years [23-37]. However, systematic methods and more accurate prediction are still in pursuit as the subsurface reservoir is always a mystery.

The prediction model could be verified by laboratory test data and production data. Limited by the quality and quantity of samples, and the accuracy of test, laboratory test data can-not represent the permeability in the reservoir. Whereas the production performance is primarily controlled by the reservoir property, thus permeability prediction can be and should be examined by the dynamic production data.

In this study, we established a multiple linear regression model of grain size, porosity, and resistivity to predict the permeability of the first member of Liushagang Formation (L_1) in Weizhou 11-1N oil field, Beibuwan Basin, China. The accuracy and applicability of this prediction model is cross-checked with measured core results, and validated by the production performance, which is rarely mentioned in previous permeability predictions.

2. Reservoir data

Weizhou 11-1N oil field is located in Beibuwan Basin in the South China Sea and is a lithologic reservoir in an uplifted area. The first member of Eocene Liushagang Formation (L_1), which is the target formation of this study, is dominated by fan-delta front underwater distributary channel and shore-shallow lacustrine deposition. There are five major oil-bearing layers in L_1, namely L_1I, L_1II, L_1III, L_1IV, and L_1V from top to bottom.

2.1. Lithology and storage space

The L_1 reservoir mainly consists of conglomerate, coarse sandstone, and fine-medium sandstone, and the sandstones are primarily feldspathic quartz sandstone (Fig. **1**). The rock samples demonstrate the particle-support structure and porous cementation, and the size-sorting is of medium deviation. The cement are generally argillaceous, carbonates and silicate (secondary enlargement). The storage space of L_1 is dominated by residual primary inter-granular pores and a small amount of inter-granular dissolution pores and feldspar dissolution pores; a few intra-granular dissolution pores and matrix micro pores develop as well (Fig. **2**).

Mercury injection experiment has been conducted on 23 samples to study the storage space characteristics. The pore-throat size converted from mercury pressure indicates the pores and throats can be clearly discriminated. The maximum connected throat diameter ranges 6.14~180 μm, with the averaged value of 55μm; the median throat diameter ranges 0.71~29.01 μm, averaged at 8.97μm (Table **1**), demonstrates favourable storage capacity.

The reservoir demonstrates strong heterogeneity, rapid sand body phase change, weak edge-bottom water power and small natural water invasion. Flooding exploitation was implemented at the early production stage for the oil field to keep the formation pressure, while artificial lift production is implemented currently.

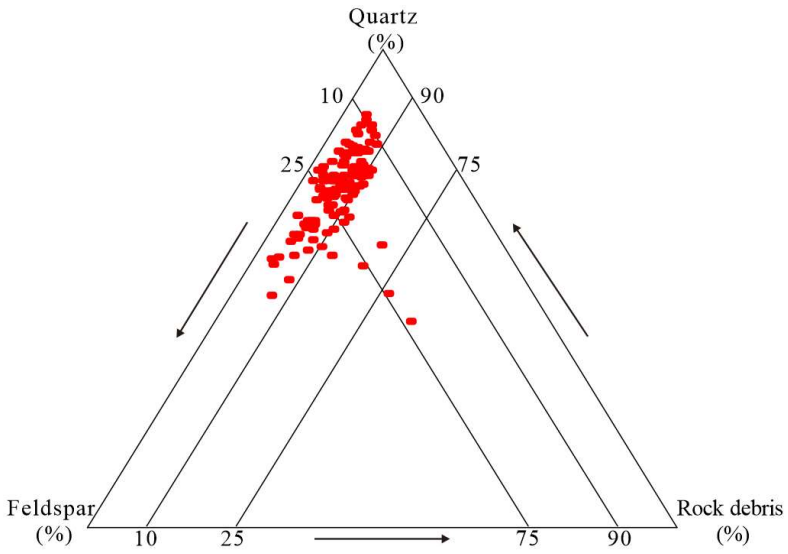

Figure 1: The sandstone types of L1 reservoir.

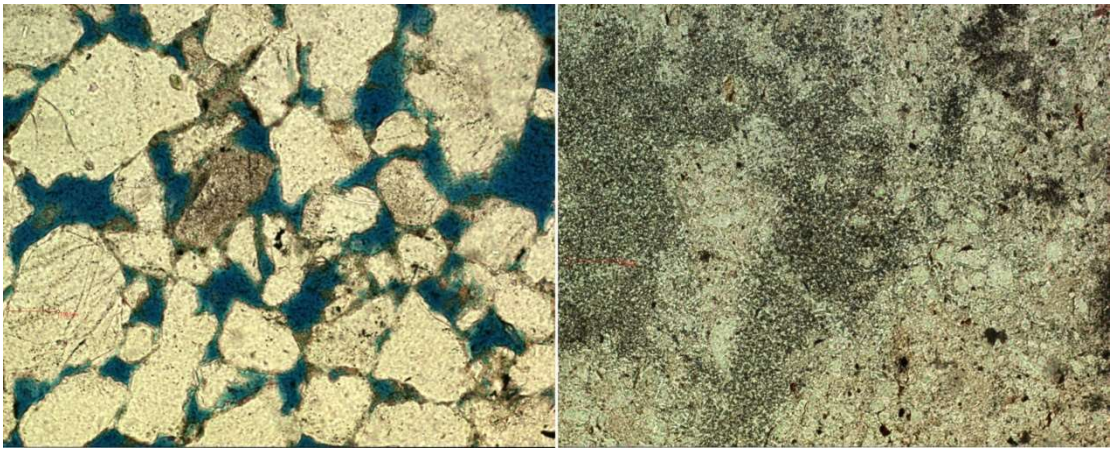

Figure 2: Images of pores in L_1 reservoir samples from casting thin sections (left: intra-granular and inter-granular dissolution pores; right: micro pores in matrix).

Table 1: Reservoir property from mercury injection (symbol definitions in the Nomenclature)

Value	Porosity %	Permeability $10^{-3}\mu m^2$	P_d MPa	P_{50} MPa	R_{50} μm	S_{max} %	S_{hgr} %	W_e %
Max	26.71	5834.61	0.046	1.036	29.01	96.11	82.11	35.37
Min	17.12	93.01	0.004	0.025	0.71	89.07	60.94	10.11
Mean	22.01	2217.23	0.016	0.160	14.20	92.36	74.31	19.49

Table 2: Lithology and physical property of effective reservoir in Weizhou Oilfield

Formation	Fluid	Lithology	Effective Porosity (%)	Permeability (mD)	Oil saturation (%)
L_1	oil	Sand-conglomerate sandstone	≥12	≥5.8	≥35

2.2. Porosity and permeability

Porosity and permeability are tested for 523 core samples of L_1 reservoir from 6 wells in Weizhou 11-1N Oil Field.

Measured porosity of L_1 in this area mainly distributes in a single peak with the range of 12%~24% (Fig. **3a**). Porosity within this range sum up to 85% of all samples; as listed in Table **2**, the threshold of effective porosity is set 12%.

Measured permeability of L_1 in this area displays single-peak distribution. The values range 10~2000 mD, and over 40% of the permeability is around 10 mD (Fig. **3b**). The threshold of effective permeability is set 5.8 mD.

The measured porosity and permeability demonstrate the L_1 reservoir is mesoporous and medium-high permeable reservoir, and can be categorized as good reservoir.

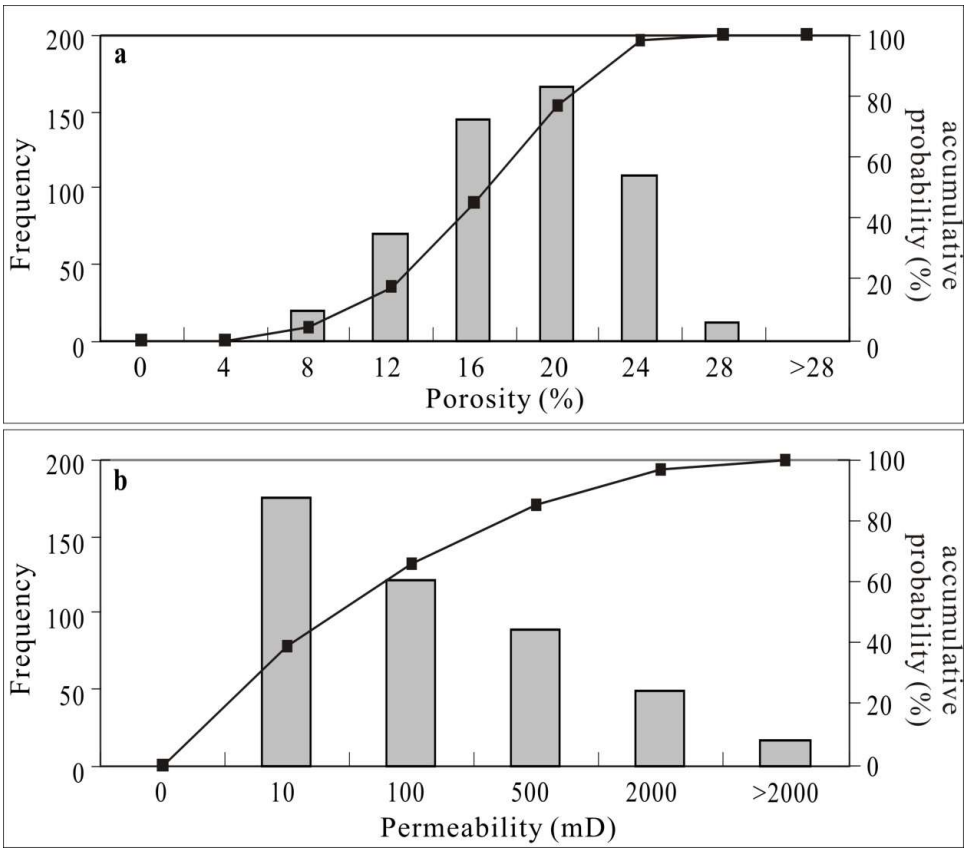

Figure 3: Porosity and permeability distribution histogram of L_1 core samples.

Porosity and permeability vary greatly over different lithologies. Porosity in pebbly sandstone and coarse sandstone ranges 12%~28%, with permeability ranges 100~10000 mD; while in siltstone and fine-medium sandstones, porosity and permeability ranges 14%~24% and 100~1000 mD, respectively (Fig. **4**). Overall, the reservoir property turns to be better with the coarsening of grain size.

2.3. Current status of permeability prediction

Porosity is a key parameter to estimate permeability in petroleum engineering practice. Porosity correlates positively with permeability in most cases. However, there may probably be a wide range of permeability correlating to one specific porosity value due to the complexity of pore structures. As in Fig. **6**, the cross plot of porosity and permeability of L_1 reservoir samples shows a generally positive relationship, but permeability varies

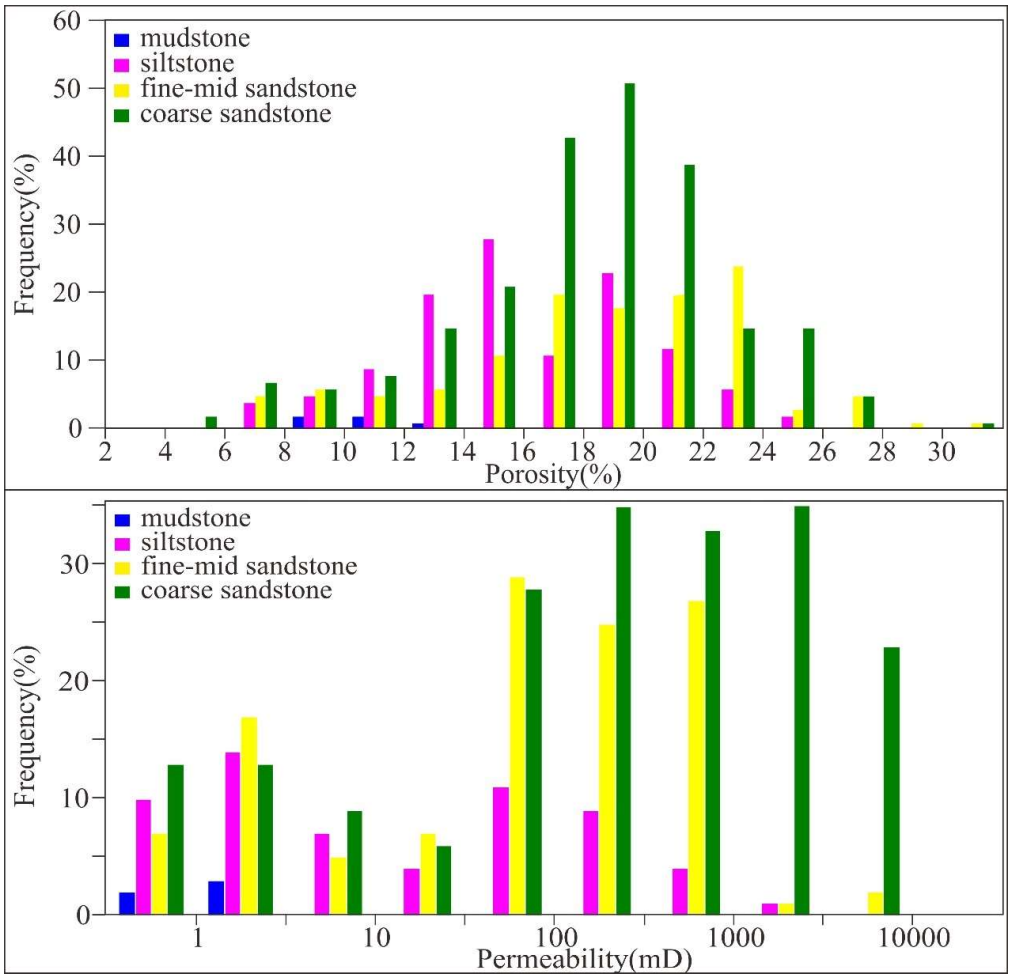

Figure 4: Porosity and permeability of different lithologies.

over orders of magnitude at the same porosity value (Fig. **5**). Therefore leaning on porosity solely cannot lead to accurate permeability prediction. More parameters need to be considered to get a more reliable permeability prediction for reservoir evaluation and production planning.

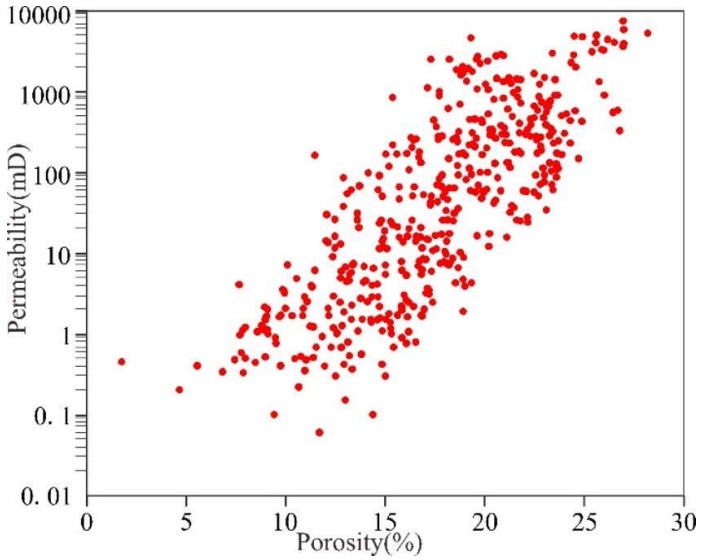

Figure 5: Scatter diagram of porosity and permeability of L1 reservoir samples.

3. Method

As permeability can have direct reflections in production performance, we use static data to build a prediction model of permeability, then validate the prediction results by dynamic data.

3.1. Interpretation of static parameters

Grain size, porosity, and pore structure are the dominant static parameters controlling permeability. Marine core samples are even more difficult to get hence few test data can be obtained, but they can be estimated through the analysis of corresponding features of common well logs.

3.1.1. Grain size (median grain diameter, M_d)

As shown in Fig. (**4**), the reservoir property demonstrates a positive relationship with grain size in this clastic reservoir. In this study, median grain diameter (M_d), which is the median value of grain size in sandstone reservoir, is employed to estimate permeability. While core samples are discontinuous and not easy to get, well logging corresponding patterns are used to determine the M_d. In this study, the M_d values of 25 core samples are correlated to the well logs at the same depths. Based on these correlations, density (ρ), neutron (γ), and gamma (GR) logs are selected to establish a calculation model for Md. The model is presented as following:

$$M_d = 0.001\gamma^3 + 4.089 \times \rho^3 - 0.095 \times \gamma^2 - 17.723 \times \rho^2 + 0.002 \times GR^2 + 2.497 \times \gamma + 18.775 \times \rho - 0.346 \times GR \quad (1)$$

in which M_d: median grain diameter

γ: value of neutron log

ρ: value of density log

GR: value of gamma-ray log

3.1.2. Porosity (Φ)

Neutron density logging has been carried out for all the wells in Weizhou 11-1N Oil Filed. After the quality control and additive correction of neutron density curves, the neutron-density intersection method in Geo frame Petroview Plus module has been done to calculate the porosities in L_1 reservoir in this area.

3.1.3. Pore structure indicator (resistivity, R)

Pore-throat diameter is the key factor determining the pore structures [38, 39]. Though the pore throat diameter could not be directly interpreted by well logs, the value of water saturation can be used to indirectly evaluate the pore-throat diameter. The Simandoux equation [40] is commonly used for estimating the water saturation of sandstones with shale content:

$$Sw = \sqrt{\frac{a \times Rw}{Rt \times \Phi^m}} - Vsh \times \frac{Rw}{0.4 \times Rsh} \quad (2)$$

in which Sw: water saturation

Rw: formation water resistivity, Ω·m

Rt: true resistivity of the formation, Ω·m;

Φ: porosity, f

Vsh: shale content, f

Rsh: shale resistance, Ω·m

a: lithology coefficient, constant

m: cementation index, constant

3.2. Nonlinear regression method

When the three parametersΦ, M_d, R are determined, these parameters are correlated with measured permeability to build a nonlinear regression model.

3.3. Validation using dynamic data

We use the predicted permeability k to calculate the formation coefficient (kH), which is the multiplication of the effective reservoir thickness and effective permeability, the kH portion, which is the portion of the kH of specific layer out of all layers in a well, productivity test data, production log (PLT) profiles to validate the accuracy of permeability prediction.

4. Results

Permeability is controlled by the grain size, porosity, and pore structure. Multiple parameters are investigated and evaluated to appropriately represent the three controlling factors mentioned above, and a prediction model using these parameters is established.

4.1. Interpretation results of Static parameters

The grain size, porosity, and pore structure indicator are not always convenient, but they can be estimated through the analysis of corresponding features of common well logs.

4.1.1. M_d

Grain size interpreted from well logs fits well with the measured ones (Fig. **6**), indicating the model is applicable in this area.

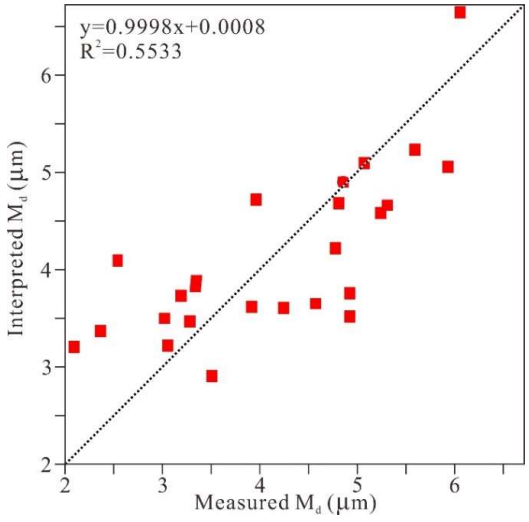

Figure 6: Cross-plot of interpreted and measured median grain diameters (M_d).

4.1.2. Φ

The porosity interpreted from neutron density log is consistent with the core porosity (Fig. **7**). Most of the points are in a range with relative error smaller than 8% (average error is 0.3%), which is acceptable in reserve calculation.

4.1.3 R

The water saturation is supposed to be a parameter for permeability prediction along with Md and porosity. But as porosity is already a stand-alone parameter, it will be redundant to use porosity again in water saturation

calculation. Therefore the resistivity (R) is taken as the third parameter instead of the water saturation to keep the model concise and avoid redundant computation. In this study, the P_{16H} log is selected to represent the resistivity.

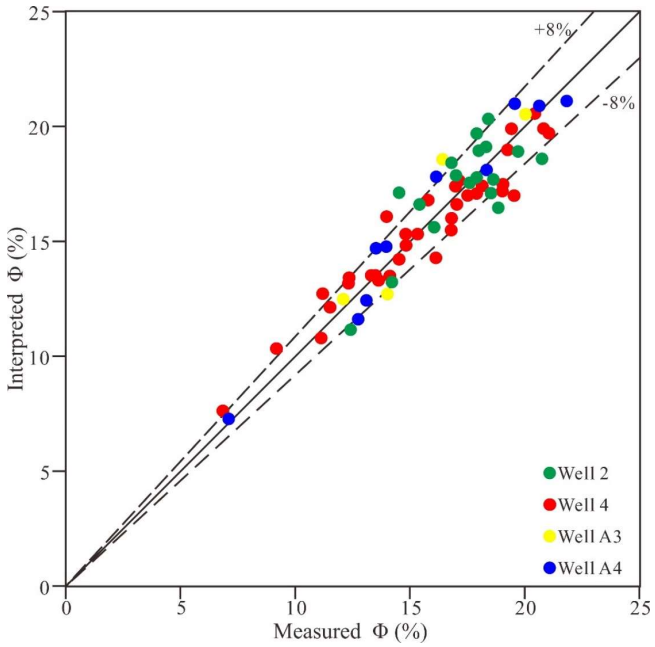

Figure 7: Comparison of interpreted porosity and core porosity in Weizhou 11-1N Oil Field (different colors represent different wells).

4.2. Static-data based permeability prediction model

As the three parametersΦ, M_d, R are determined, these parameters are correlated with measured permeability (Fig. **8**). Permeability demonstrates a positive correlation with porosity, while a negative correlation with resistivity. Though there is no clear trend between permeability and grain size, grain size is still taken as a parameter considering the significance of pore-throat structure.

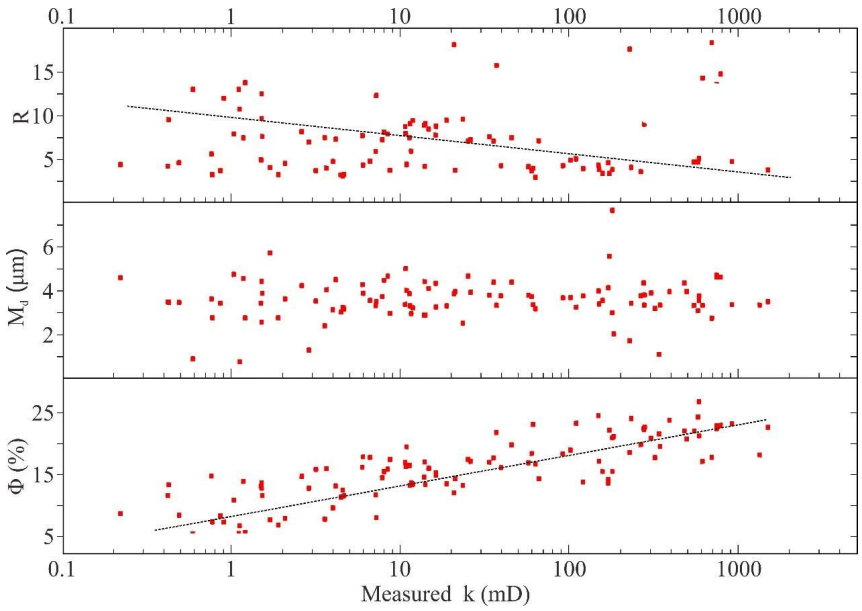

Figure 8: Scatter diagram of permeability with porosity (Φ), grain size (M_d), and resistivity (R).

Based on the understanding of reservoir physical property and characteristics of the cross plot of the parameters, curve estimation has been carried out between the parameters and permeability with SPSS software. The permeability prediction model is eventually established after fitting of single parameter and non-linear analysis of multiple parameters. It is assigned in the permeability model the interpreted permeability equals 3 when it is unreasonable (smaller than 1 mD):

$$K = -27.7 \times {M_d}^{-5.8} + 2.1 \times 10^{-4} \times \Phi^{4.7} + 10 \times R^{-0.5} \quad (3)$$

$$K = \begin{cases} K \leq 1, K = 3 \\ K > 1, K \end{cases}, \ R^2 = 0.408$$

In which k: permeability, mD

M_d: median grain diameter, calculated from equation (1), μm

Φ: porosity, calculated from the neutron-density method

R: resistivity, P_{16H} log in this area

5. Discussion

The permeability implied in dynamic production data (obtained from formation test and production) is more reliable and closer to the "true" permeability of the reservoir, and could be used to calibrate the permeability prediction together with core test data. Thus, the accuracy and applicability of the permeability prediction model are double-checked by the laboratory test data and production performance.

5.1. Accuracy evaluation of permeability prediction

The permeability calculated from the prediction model fits well with the core test data from the well profile and the cross plot (Figs. **9**, **10**). The predicted permeability is mostly greater than the measured permeability. This phenomenon might have been caused by errors in porosity calculation. The neutron-density method gives a result of bulk porosity, which is always greater than effective porosity.

5.2. Validation of permeability estimation by dynamic production performance

Formation coefficient (kH), which is the multiplication of the effective reservoir thickness and effective permeability, can be used to determine the production allocation proportion of the oil-bearing layers of the wells. The kH portion is the portion of the kH of a specific layer out of all layers in a well, which represents the weight of this layer among all production layers. The comparison of production allocation proportion and productivity data or production log (PLT) profiles could then validate the accuracy of permeability prediction. The results of kH portion, productivity test, and PLT of 6 representative wells are listed in Table **3** and Fig. **11**.

The kH portion and productivity are much the same within each oil-bearing layer. Considering the effective thickness of the oil layers does not vary much between wells, the correlation can be stated as oil layers with better productivity are with better porosity and permeability. This conclusion indicates the predicted permeability is appropriate.

When correlated with the productivity index and water absorption index, good reservoir quality tends to yield better productivity and water injection performance (Table **4**). Well A3 and A4 are with better porosity and permeability than Well A2, A5, and A6, accordingly the productivity index is better of the former two wells than of the other three. This correlation demonstrates reservoirs with better porosity and permeability has more favourable production ability than those with the poor property. This conclusion is consistent with common sense, proving the predicted permeability is reliable.

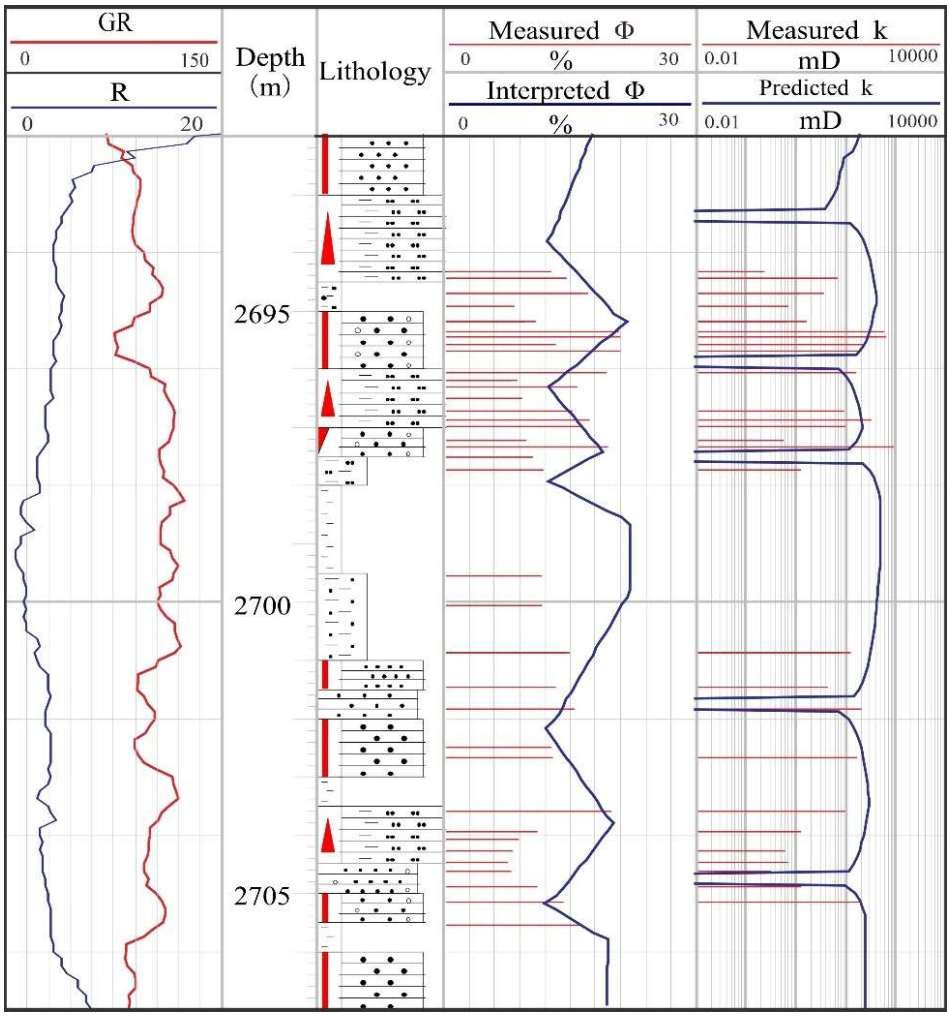

Figure 9: Profile of Well A3.

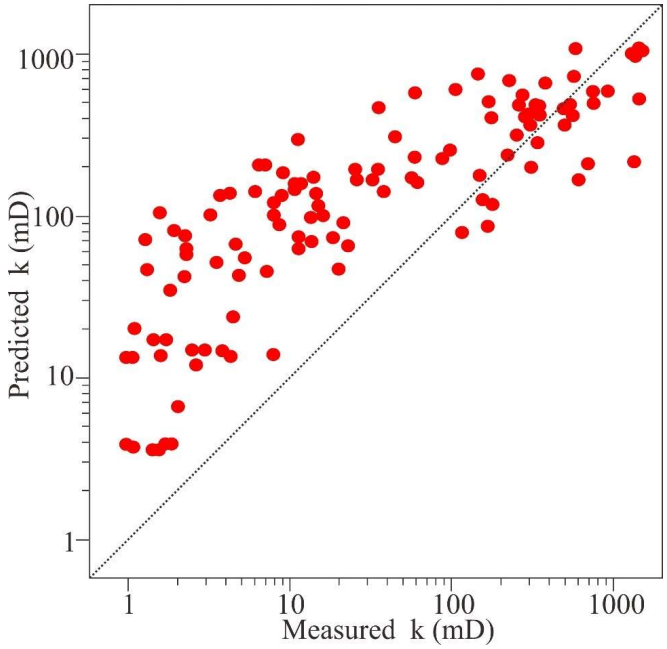

Figure 10: Crossplot of core permeability and predicted permeability.

Table 3: Formation coefficient (kH), productivity test and PLT data of selected wells

Well	Oil-bearing layer	kH	kH portion (%)	Productivity (%)	PLT (%)
A1	L_1I	32333	86.79	90.52	78.45
	L_1III	1602	4.30	3.74	11.12
	L_1IV	1985	5.33	4.35	10.43
	L_1V	1335	3.58	1.39	0.00
A2	L_1I	13657	67.44	71.05	58.30
	L_1II	2171	10.72	15.04	17.35
	L_1IV	4421	21.83	13.91	24.34
A4	L_1II	4623	59.59		77.24
	L_1IV	3234	40.40		22.76
A5	L_1II	3225	39.08	44.35	38.27
	L_1IV	5027	60.92	55.65	61.73
A6	L_1II	2565	74.09	80.93	80.46
	L_1V	897	25.91	19.07	19.54

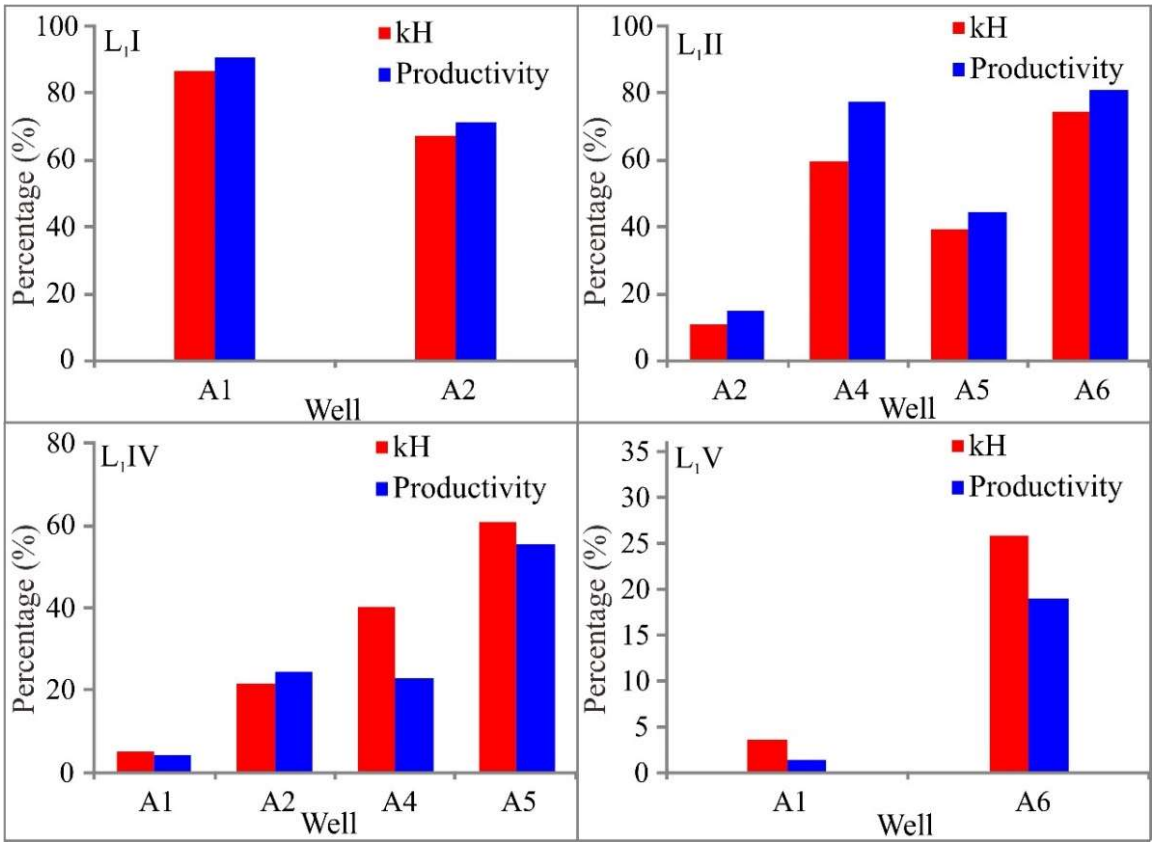

Figure 11: Comparison of kH and productivity in different oil-bearing layers (There is only one set of data for L1III and the kH is close to the productivity; In Well A4 there is no productivity test so the PLT data is adopted to demonstrate the consistency of kH and production performance.)

Table 4: Comparison of physical property and Liquid production/water absorption capability estimation of L_1 II oil layer

Well	Thickness m	Porosity %	Permeability (mD)			Productivity index $m^3/(MPa·d·m)$	Water absorption index $m^3/(MPa·d·m)$
			Ave.	Min.	Max.		
A2	12.3	13.7	73.8	3.0	373.4	0.20	
A3	27.9	16.9	148.4	3.0	1031.8	1.11	
A4	21.7	15.4	135.6	3.0	819.2	0.95	
A5	38.7	14.9	105.9	3.0	365.3	0.47	
A6	41.4	14.2	81.1	3.0	265.9	0.62	
A8	24.9	12.8	53.8	3.0	343.5		4.42
A9	30.9	16.3	125.7	3.0	276.1		29.40
A10	23.4	12.3	46.9	3.0	204.9		10.55
A11	16.7	13.0	122.0	73.5	157.8		24.20
A13	25.6	17.0	154.5	3.0	356.5		27.97

5. Conclusion

(1) Grain size, porosity and resistivity can be employed to predict the permeability of L_1 reservoir in Weizhou 11-1N Oil Field. The prediction result is consistent with the laboratory test data and production performance. The permeability model is accurate and applicable in this area and bridges the geological parameters and production performance.

(2) Multiple linear regression, instead of a single parameter (porosity), is more reasonable and practical in permeability analysis. But it is noteworthy that the multiple linear regression model for permeability prediction should be constrained by actual geological factors and validated by the production performance.

Nomenclature

P_d: Displacement pressure

P_{50}: Mercury saturation median pressure

R_{50}: Median pore radius

S_{max}: maximum injected mercury saturation

S_{hgr}: remaining mercury saturation

W_e: mercury withdraw efficiency

M_d: median grain diameter, μm

Φ: porosity, f or %

γ: value of neutron log

ρ: value of density log

GR: value of gamma ray log

k: permeability, mD (1mD≈0.987×10^{-3}μm^2)

kH: the multiplication of the effective reservoir thickness and effective permeability

References

[1] Wyckoff, R.D, Botset, H.G., Muskat, M., 1933. The measurement of the permeability of porous media for homogeneous fluids. Review of Scientific Instruments, 4(7): 394-405.

[2] Martin, M., Murray, G.H., Gillingham, W.J., 1938. Determination of the potential productivity of oil-bearing formations by resistivity measurements. Geophysics, 3(3): 258-272.

[3] Archie, G.E., 1942. The electrical resistivity log as an aid in determining some reservoir characteristics. Transactions of the AIME, 146(1): 54-62.

[4] Brace, W.F., 1977. Permeability from resistivity and pore shape. Journal of Geophysical Research, 82(23): 3343-3349.

[5] Jackson, P.D., Smith, D.T., Stanford, P.N., 1978. Resistivity-porosity-particle shape relationships for marine sands. Geophysics, 43(6): 1250-1268.

[6] Katz, A.J., Thompson, A.H., 1985. Fractal sandstone pores: implications for conductivity and pore formation. Physical Review Letters, 54(12): 1325.

[7] Katz, A.J., Thompson, A.H., 1986. Quantitative prediction of permeability in porous rock. Physical review, 34(11): 8179.

[8] de Lima, O.A.L., 1995. Water saturation and permeability from resistivity, dielectric, and porosity logs. Geophysics, 60(6): 1756-1764.

[9] Fowles, J., Burley, S., 1994. Textural and permeability characteristics of faulted, high porosity sandstones. Marine and Petroleum Geology, 11(5): 608-623.

[10] Mohaghegh, S., Balan, B., Ameri, S., 1995. State-of-the-art in permeability determination from well log data: Part 2-verifiable accurate permeability predictions the touch-stone of all models. Society of Petroleum Engineers.

[11] Mohaghegh, S., Arefi, R., Bilgesu, I., 1995. Design and development of an artificial neural network for estimation of formation permeability. SPE Computer Applications, 7(6): 151-154.

[12] Saner, S., M. Kissami, S. AlNufaili. 1997. Estimation of permeability from well logs using resistivity and saturation data. SPE Formation Evaluation, 12(1): 27-31.

[13] Xue, G.P., DattaGupta, A., Valko, P., 1997. Optimal transformations for multiple regression: Application to permeability estimation from well logs. SPE Formation Evaluation, 12(2): 85-93.

[14] Yang, Y., Aplin, A.C., 1998. Influence of lithology and compaction on the pore size distribution and modelled permeability of some mudstones from the Norwegian margin. Marine and Petroleum Geology, 15(2): 163-175.

[15] Cuddy, S. J., 2000. Litho-facies and permeability prediction from electrical logs using fuzzy logic. SPE Reservoir Evaluation & Engineering, 3(4): 319-324.

[16] Bhatt, A., Helle, H.B., 2002. Committee neural networks for porosity and permeability prediction from well logs. Geophysical Prospecting, 50(6): 645-660.

[17] Lee, S.H., Kharghoria, A., Datta-Gupta, A., 2002. Electrofacies characterization and permeability predictions in complex reservoirs. SPE Reservoir Evaluation & Engineering, 5(3): 237-248.

[18] Perez, H.H., Datta-Gupta, A., Mishra, S., 2005. The Role of Electrofacies Lithofacies and Hydraulic Flow Units in Permeability Predictions from Well Logs: A Comparative Analysis Using Classification Trees. SPE Reservoir Evaluation & Engineering, 8(2): 143-155.

[19] Rezaee, M.R., Jafari, A., Kazemzadeh, E., 2006. Relationships between permeability, porosity and pore throat size in carbonate rocks using regression analysis and neural networks. Journal of Geophysics and Engineering, 3(4): 370-383.

[20] Shokir, E.M., Alsughayer, A.A., Al-Ateeq, A., 2006. Permeability estimation from well log responses. Journal of Canadian Petroleum Technology, 45(11): 41-46.

[21] Al-Anazi, A., Gates, I.D., 2010. Support-Vector Regression for Permeability Prediction in a Heterogeneous Reservoir: A Comparative Study. SPE Reservoir Evaluation & Engineering, 13(3): 485-495.

[22] Tahar, A., Baouche, R., Baddari, k., 2014. Neuro-fuzzy system to predict permeability and porosity from well log data: A case study of Hassi R'Mel gas field, Algeria. Journal of Petroleum Science and Engineering, 123: 217-229.

[23] Chehrazi, A., Rezaee, R., 2012. A systematic method for permeability prediction, a Petro-Facies approach. Journal of Petroleum Science and Engineering, 82: 1-16.

[24] Jesús, D.C., Biosca, B., Miguel, M.J., 2015. Geophysical estimation of permeability in sedimentary media with porosities from 0 to 50%. Oil & Gas Science and Technology-Revue d'IFP Energies nouvelles, 71(2): 27-35.

[25] Fitch, P.J.R, Lovell, M.A, Davies, S.J., 2015. An integrated and quantitative approach to petrophysical heterogeneity. Marine and Petroleum Geology, 63: 82-96.

[26] Rosenbrand, E., Fabricius, I.L., Fisher, Q., 2015. Permeability in Rotliegend gas sandstones to gas and brine as predicted from NMR, mercury injection and image analysis. Marine and Petroleum Geology, 64: 189-202.

[27] Taylor, T.R., Kittridge, M.G., Winefield, P., 2015. Reservoir quality and rock properties modeling - Triassic and Jurassic sandstones, greater Shearwater area, UK Central North Sea. Marine And Petroleum Geology, 65: 1-21.

[28] Zhu, L.Q., Zhang, C., Wei, Y., Zhang, C.M., 2017. Permeability Prediction of the Tight Sandstone Reservoirs Using Hybrid Intelligent Algorithm and Nuclear Magnetic Resonance Logging Data. Arabian Journal for Science and Engineering, 42(4): 1643-1654. doi:10.1007/s13369-016-2365-2

[29] Ju, W., Wu, C.F., Wang, k., Sun, W.F., Li, C., Chang, X.X., 2017. Prediction of tectonic fractures in low permeability sandstone reservoirs: A case study of the Es-3(m) reservoir in the Block Shishen 100 and adjacent regions, Dongying Depression. Journal of Petroleum Science and Engineering, 156: 884-895. doi:10.1016/j.petrol.2017.06.068

[30] Wang, J., Cao, Y.C., Liu, k.Y., Liu, J., Kashif, M., 2017. Identification of sedimentary-diagenetic facies and reservoir porosity and permeability prediction: An example from the Eocene beach-bar sandstone in the Dongying Depression, China. Marine and Petroleum Geology, 82: 69-84. doi:10.1016/j.marpetgeo.2017.02.004

[31] Liu, M., Xie, R.H., Wu, S.T., Zhu, R.k., Mao, Z.G., Wang, C.S., 2018. Permeability prediction from mercury injection capillary pressure curves by partial least squares regression method in tight sandstone reservoirs. Journal of Petroleum Science and Engineering, 169: 135-145. doi:10.1016/j.petrol.2018.05.020

[32] Ngo, V.T., Lu, V.D., Le, V.M., 2018. A comparison of permeability prediction methods using core analysis data for sandstone and carbonate reservoirs. Geomechanics and Geophysics for Geo-Energy and Geo-Resources, 4(2): 129-139. doi:10.1007/s40948-017-0078-y

[33] Ojo, S.A., Ozebo, V.C., Olusola, O.I., Olatinsu, O.B., 2018. Continuous permeability predictions in heterogeneous reservoirs using Vshale and microstructure calibrated free-fluid models(a combined study of a Niger Delta field and the tight gas sandstone of the southern North Sea). Arabian Journal of Geosciences, 11(17): 527. doi:10.1007/s12517-018-3879-6

[34] Lis-Sledziona, A., 2019. Petrophysical rock typing and permeability prediction in tight sandstone reservoir. Acta Geophysica, 67(6): 1895-1911. doi:10.1007/s11600-019-00348-5

[35] Rostami, S., Rashidi, F., Safari, H., 2019. Prediction of oil-water relative permeability in sandstone and carbonate reservoir rocks using the CSA-LSSVM algorithm. Journal of Petroleum Science and Engineering, 173: 170-186. doi:10.1016/j.petrol.2018.09.085

[36] Baouche, R; Nabawy, BS, 2021. Permeability prediction in argillaceous sandstone reservoirs using fuzzy logic analysis: A case study of triassic sequences, Southern Hassi R'Mel Gas Field, Algeria. Journal of African Earth Sciences, 173: 104049. doi:10.1016/j.jafrearsci.2020.104049

[37] Zhang, G.Y., Wang, Z.Z., Mohaghegh, S., Lin, C.Y., Sun, Y.N., Pei, S.J., 2021. Pattern visualization and understanding of machine learning models for permeability prediction in tight sandstone reservoirs. Journal of Petroleum Science and Engineering, 200: 108142. doi:10.1016/j.petrol.2020.108142

[38] Tsakiroglou, C.D., Payatakes, A.C. 2000. Characterization of the pore structure of reservoir rocks with the aid of serial sectioning analysis, mercury porosimetry and network simulation. Advances in Water Resources, 23(7): 773-789.

[39] Clarkson, C.R, Solano, N., Bustin, R.M., 2013. Pore structure characterization of North American shale gas reservoirs using USANS/SANS, gas adsorption, and mercury intrusion. Fuel, 103: 606-616.

[40] Simandoux, P., 1963. Dielectric measurements of porous media: Application to measurement of water saturations-study of the behavior of argillaceous formations. Revue de L'institut Francais du Petrole, 18(S1): 193-215.